International Journal of Engineering Trends and Technology
ISSN: 2231–5381 / https://doi.org/10.14445/22315381/IJETT-V73I7P123

Volume 73 Issue 7, 293-307, July 2025

Original Article

Synthesis, Thermal, Hirschfeld Surface Analysis, and Spectroscopic Properties of a Cd(II) Coordination Polymer with 1-Hydroxy-2-Naphthoic Acid

D.Kh. Saidov[1], Kh.Kh. Turaev[2], A.B. Ibragimov[3], G.Kh. Toirova[4], Kh.Kh. Kulbasheva[5]

[1,2,4]*Termiz State University, Faculty of Chemistry, Termez, Uzbekistan.*
[3]*Institute of General and Inorganic Chemistry, Academy of Sciences of Uzbekistan, Tashkent, Uzbekistan.*
[5]*Denau Entrepreneurship and Pedagogy Institute, Denau, Uzbekistan*

[3]*Corresponding Author : saidovdilmurod@514gmail.com*

Received: 02 April 2025 Revised: 21 June 2025 Accepted: 30 June 2025 Published: 30 July 2025

Abstract - *In this paper, a new cadmium-based polymer was synthesized using 1-hydroxy-2-naphthoic Acid and cadmium acetate. The structural and physicochemical properties of the obtained polymer were investigated using various analytical techniques. Moreover, Hirshfeld surface analysis was employed to assess intermolecular interactions, while FT-IR and UV-Vis spectroscopy provided insights into the functional groups and electronic transitions. Thermal behavior was examined through Differential Thermal Analysis (DTA) and thermogravimetric analysis (TGA). The crystallinity and phase purity were confirmed by X-Ray Diffraction (XRD) using a Rigaku MiniFlex 600 diffractometer. In addition, elemental composition was determined via CHNS/O analysis (Thermo Scientific FlashSmart), and morphological studies were conducted using scanning electron microscopy (SEM) and energy-dispersive X-ray spectroscopy (EDS). Additionally, the polymer's electrical properties were evaluated through conductometric measurements.*

Keywords - *Cadmium-based polymer, 1-hydroxy-2-naphthoic Acid, Hirshfeld surface analysis, FT-IR, UV-Vis, XRD, DTA, TGA, CHNS/O analysis, SEM-EDS, Conductometry.*

1. Introduction

In recent years, the synthesis of new coordination polymers has increased [1]. Metal-organic frameworks (MOFs) are crystalline compounds with a highly ordered structure. They comprise one or more metal ions or metal clusters, which combine using multifaceted organic groups-binders, forming bonds. These branches constitute the main structure of the polymer. These binders act as bridges between branches and ensure the porosity of metal-organic frames or polymers [2]. Metal-organic frameworks with permanent porosity were first identified in the late 20th century and have attracted widespread scientific interest over the past 20-30 years due to their unique properties such as porosity, tunable functionality, and structural diversity [3]. The diversity of polymers is studied to encompass gas storage, separation, catalysis, luminescence, sensing, proton conduction, electron conduction, and energy conversion [4]. If MOFs have a clearly defined porosity, metallic composition, and a specific crystalline structure, polymers can be processed mechanically and have chemical resistance. Since MOFs have a large surface area, a clearly defined porous structure, and contain metal ions, they are particularly important in gas adsorption or catalysis. In this way, it will be possible to preserve many molecules [5]. Due to the remarkable properties and diversity of samples, polymers are utilised for various purposes in numerous industries and research fields [6]. During the synthesis of 2D polymers in single crystals, external action (mainly light) layered monomer crystals regularly transform into a crystal consisting of covalently bonded layers [7]. Two-dimensional polymers (2D) are macromolecular sheets that combine permanent porosity with long-range order. This periodicity enables the deterministic placement of chemical functionality in porous organic materials [8]. 2D MOFs have been synthesised from organic ligands and metal salts, enabling full utilisation of MOF advantages in electrocatalysis. After exfoliation, 2D MOFs exhibit higher electrocatalytic activity than bulk MOFs due to their larger specific surface area and increased reactivity, contributing to improved electrocatalytic performance [9]. In addition, the ultra-thin structure of 2D MOFs contributes to an increase in ion and electron transfer rate in the electrocatalytic process due to the opening of many oxidation-reduction active centres and a reduction in the diffusion distance. At the same time, traditional volumetric MOFs have low electrical conductivity [10, 11]. On the other hand, in two-dimensional MOFs, two-dimensional elongated organic sheets are arranged layer by

layer, forming periodic columnar π-structures. This makes them excellent candidates with photoelectric properties and thus expands their range of biomedical applications. According to results, MOFs can be used not only as a drug carrier but also for cancer treatment by phototherapy and therapeutic methods [12]. Self-assembled Metal Coordination Complexes (MCC) from metal ions and organic ligands with multiple binding sites have attracted widespread attention due to their unique structure and potential applications in scientific fields such as photoluminescence [13], sensors [14], separation [15] and storage [16], catalysis [17], energy [18], and magnetism [19]. These complexes are deeply studied by scientists and applied in various fields. Thus, to create new Metal-Coordination Complexes (MCCs) with specific structural motifs, an organic binder of 1-hydroxy-2-naphthoic Acid was developed and tested. As a result, this new semi-solid 1-hydroxy-2-naphthoic Acid, the search and study of MCCs containing organic ligands, is an unexplored area. [20]. Normally, cadmium-based MCCs are available, and they have been shown to have excellent luminescent properties [21]. 1-Hydroxy-2-naphthoic Acid is used as an intermediate for azo and triphenylmethane dyes and, more recently, for colour film dyes [22]. Complexes of many p-, d-, and 4f-metals with 1-hydroxy-2-naphthoic Acid are currently known in the literature [23]. In addition to its use in organic synthesis, [24]. 1-Hydroxy-2-naphthoic Acid has found many other applications, such as an intermediate for the production of long-life batteries. The sodium salt of 1-hydroxy-2-naphthoic Acid is commonly used to dissolve riboflavin. It can also be used in biochemical studies to determine the content of ammonium, magnesium, and potassium. In this study, the composition and structure of the polymer were studied more deeply than in previous works. According to the results of Thermogravimetric Analysis (TGA), it was found that ligand L1 retains thermal stability up to 592.85°C, which will allow the synthesis of heat-resistant sorption Metal-Organic Frameworks (MOFs) based on this ligand in the future.

The main aim of this work is to study the new Cd(II) coordination polymer based on 1-hydroxy-2-naphthoic Acid. And its structure and other properties are studied using modern physicochemical methods.

2. Experimental Part

2.1. Methods

The structural and physicochemical properties of the ynthesised polymer were assessed by complex instrumental analysis. Hirschfeld surface analysis was used for the visual and quantitative analysis of intermolecular interactions in the crystal structure. X-ray diffraction (Rigaku MiniFlex 600) was used to determine the degree of crystallinity and phase composition. Thermal stability and decomposition processes were studied using TGA/DTA. UV-Vis spectroscopy was used to determine electronic transitions and optical properties. CHNS/O analysis confirmed the completeness of the synthesis by determining the elemental composition. Superficial morphology was assessed using SEM, and the distribution of elements was assessed using EDS. Conductometry was used to determine the polymer's ionic conductivity and dissociation properties.

2.2. Materials and Methods

The compounds used in this study were cadmium acetate dihydrate salt, 1-hydroxy-2-naphthoic Acid (L1), and acetic Acid. All chemical reagents were purchased from Sigma-Aldrich as “chemical pure”.

2.3. Synthesis, Element Analysis

0.282 g (0.05 M) of 1-hydroxy-2-naphthoic Acid was dissolved in 30 ml of 96% ethanol, and the resulting solution was stirred using a magnetic stirrer for half an hour. As a result, a dark brown solution was formed. Then, after that, 0.399 g (0.05 M) of cadmium acetate dehydrate ($Cd(CH_3COO)_2 \cdot 2H_2O$) was dissolved in 20 ml of distilled water and slowly added to the prepared ligand solution and mixed thoroughly for one hour. The solution was filtered, and the filtrate turned brown. To ensure the evaporation of the solvents, the solution was stored in a thermostat at a temperature of 50–60 °C for 10 days. At the end of the process, dark brown crystals were formed. The yield was 73% (Figure 1, 2).

Calculated (in %):
C – 43.95%; H – 2.55%; O – 22.68%. Cd – 16.83%;
Found (in %):
C – 43.05%; H – 2.15%; O – 21.68%. Cd – 16.13%;

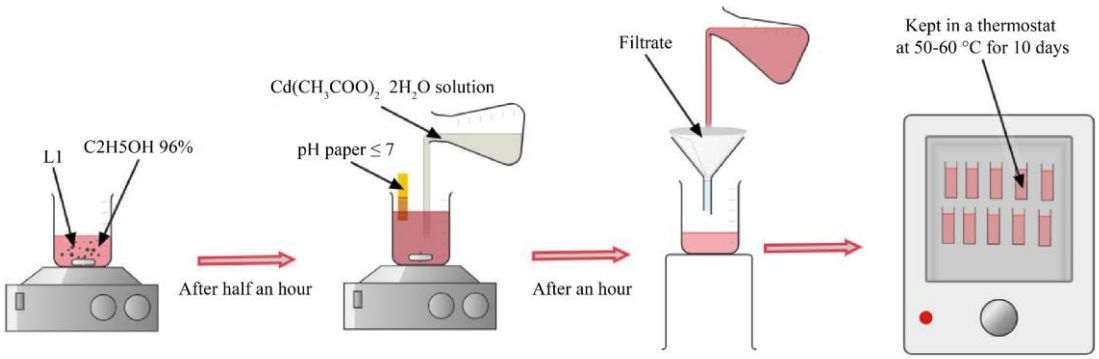

Fig. 1 Polymer crystal production scheme

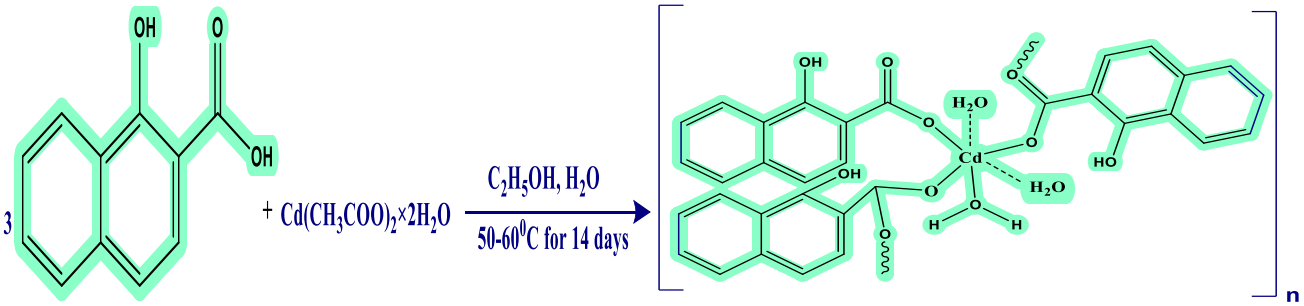

Fig. 2 Polymer synthesis reaction

3. Results and Discussion

3.1. CHNS/O Analysis

The elemental composition of the synthesised $C_{44}H_{38}Cd_2O_{18}$ polymer was analysed. This method measures the Carbon (C), Hydrogen (H), Nitrogen (N), Sulphur (S), and Oxygen (O) contents of organic and inorganic materials but cannot directly determine the amount of Cadmium (Cd).

Therefore, the C, H, and O percentages were subtracted from the total mass to determine the amount of Cd.

The carbon, oxygen, and cadmium contents are very close to the theoretical values. The largest difference was observed for hydrogen (2.82%), which is associated with moisture or losses during the synthesis process (Table 1, Figure 3).

Table 1. Comparison of theoretical and experimental elemental composition

Element	Theoretical (%)	Practical (%)	Difference (Δ%)
C(Carbon)	48.95	48.91	-0.04
H(Hydrogen)	3.55	3.65	+0.10
O(Oxygen)	26.68	26.91	+0.23
Cd (Cadmium)	20.83	100 - (48.91 + 3.65 + 26.91) = 20.53	-0.30

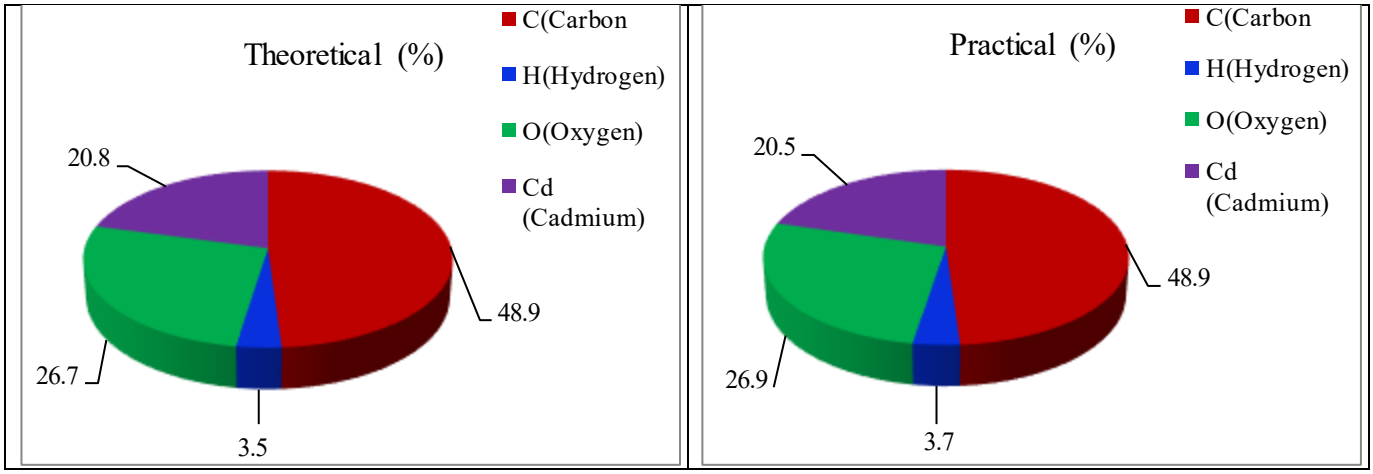

Fig. 3 Comparison of (a) Theoretical, and (b) experimental percentage composition of elements in a polymer

The obtained results confirmed the high accuracy of the elemental analysis method and showed that the composition of the synthesised polymer corresponds to the expected chemical composition. This confirms the reliability and effectiveness of the Dumas method and the CHNS/O analyser in assessing the elemental composition of the polymer. In general, the composition of the synthesised new polymer is consistent with theoretical calculations.

3.2. IR Spectrum Analysis of Polymer

The structure of the complex formed by 1-hydroxy-2-naphthoic Acid (L1) and $Cd(CH_3COO)_2 \cdot 2H_2O$ salt was analysed by Infrared (IR) spectroscopy in the range of 400–4000 cm^{-1} on a Spectrum Two (PerkinElmer) instrument (Figure 4). The obtained IR spectrum exhibited the following main characteristics: Stretching vibrations of the -OH groups in L1 and water molecules were observed at 3335 cm^{-1}, with an extended absorption range of IR radiation. Stretching vibrations of sp2-hybridised =C-H bonds in the aromatic ring were detected at 2996 cm−1, while peaks at 2602 cm−1 and 2535 cm−1 indicate the presence of a free or partially coordinated carboxyl (-COOH) group in the ligand. Strong absorptions corresponding to the stretching vibrations of the carbonyl (C=O) group were observed at 1634 cm^{-1}, while

deformation vibrations were observed at 1247 cm^{-1}.. Additionally, a broadened absorption line at 1448 cm^{-1} corresponds to the stretching vibrations of the C=C bonds in the aromatic ring. Vibrations characteristic of the complex's metal-oxygen (M-O) bonds were observed in the 603-540 cm^{1} region.

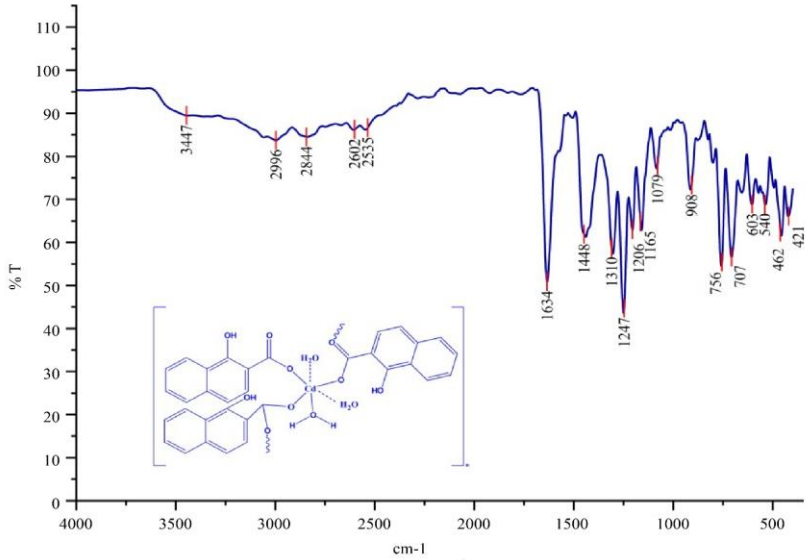

Fig. 4 IR spectrum of a complex compound

3.3. UV-Visible Spectroscopic Analysis

A 0.05 molar solution of the polymer was prepared, dissolved in C_2H_5OH (96%), and its electronic transition events were analysed (Figure 5).

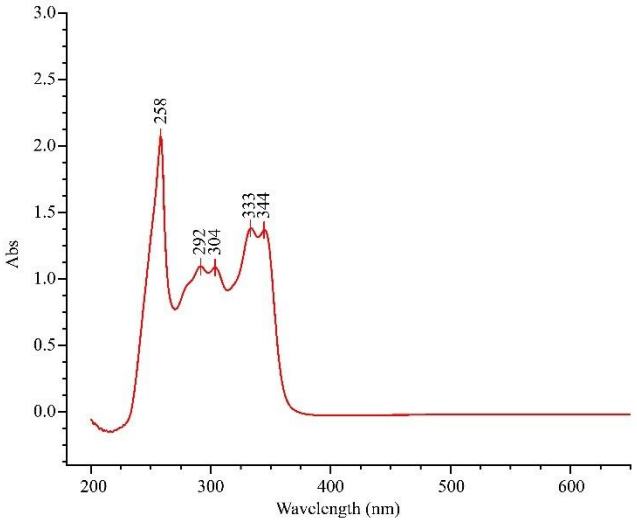

Fig. 5 UV spectrum of a polymer compound

No electronic transition events were observed in the polymer compound's Cd(II) component, resulting in no detectable signals for cadmium. A ligand-to-metal charge transfer event was observed at λ_{max} = 350 nm. Also, π-π* transitions in the aromatic ligand (1-hydroxy-2-naphthoic Acid) occurred at λ_{max} = 292, 304, 333, and 344 nm. In addition, the strong absorption peak observed at 258 nm is also associated with π-π* transitions, and the electronic system of the naphthalene ring in L1 causes intense absorption in this region.

3.3.1. Environmental Effects

The pH of the solution medium is in the range of 5-6, which affects the degree of ionization of the ligand. Under these pH conditions, the carboxyl group can partially ionize and form a strong complex compound with Cd (II) ions.

3.*4. TGA and DTA Analysis*

Thermogravimetric (TGA) and Differential Thermal Analysis (DTA) of the polymer $C_{44}H_{38}Cd_2O_{18}$ were performed (Figure 6, 7, Table 2). The measurement process was continued up to a temperature of 900ºC. For sample analysis, a polymer weighing 3.765 mg was placed in a porcelain dish, and its thermal properties were studied under the influence of temperature.

3.4.1. Thermogravimetric Analysis (TGA)

According to the results, the thermogravimetric analysis curve (TG-blue curves) shows changes in three intensive intervals. The sample underwent mass loss in three stages. The first stage mass loss began in the first minutes of thermal exposure, at 86.10ºC, and ended at 296.71ºC at 30.30 min. At this stage, the mass of MOF decreased by 46.454%, equal to 1.749 mg. Such mass loss is associated with the evaporation of water and acetic Acid contained in the outer layer of the sample. The second stage mass loss began at 296.71ºC (30.30 min) and continued until 60.49 min. During this stage, which lasted until 592.85ºC, the mass of the sample decreased by

29.668% (1.117 mg). The mass loss at this stage was due to the dissociation of the ligand (L1). In the third stage, at 901.02ºC, the sample lost 7.968% (0.3 mg) of mass. At the last stage of the process, the sample was completely decomposed, leaving cadmium oxide and organic residues.

3.4.2. Differential Thermal Analysis (DTA)

DTA analysis (red curve) showed that the heat absorption, the endothermic process, occurred in four stages. The first stage began at 14.02 min and absorbed a temperature of 135ºC. The heat absorption was completed in 17.31 min when the temperature reached 167.50ºC. Energy absorption peaked at 15.98 minutes, occurring at a temperature of 154.05°C. At this stage, -171.38 mJ (- -40.94 cal) of heat was absorbed relative to the sample mass, equivalent to 45.52 J/g (10.87 cal/g).

Simultaneously, 2.82 mV of energy was released, corresponding to 0.75 mV/mg of the sample mass. Mass loss is primarily associated with the release of adsorbed water and volatile molecules, which determines the initial thermal change of the complex. The second *stage* endothermic effect began at 17.52 minutes (169.51ºC) and ended at 20.64 minutes (200.81ºC).

The thermal energy change at this stage was 181.28 mJ. At this stage, organic components burn, forming gas, and heat-resistant molecules are released. The third *stage* endothermic effect began at 21.98 minutes (214.05ºC) and ended at 26.05 minutes (254.58ºC). The thermal energy change at this stage was -175.97 mJ. Intensive decomposition and carbonation occur in this process, resulting in the combustion of a large amount of organic matter. The last stage endothermic effect began at 38.82 minutes (380.98ºC) and ended at 56.16 minutes (550.71ºC). The change in thermal energy at this stage was 2.90 J. This stage is explained by intensive decomposition and the breaking and decomposition of 1-hydroxy-2-naphthoic acid bonds.

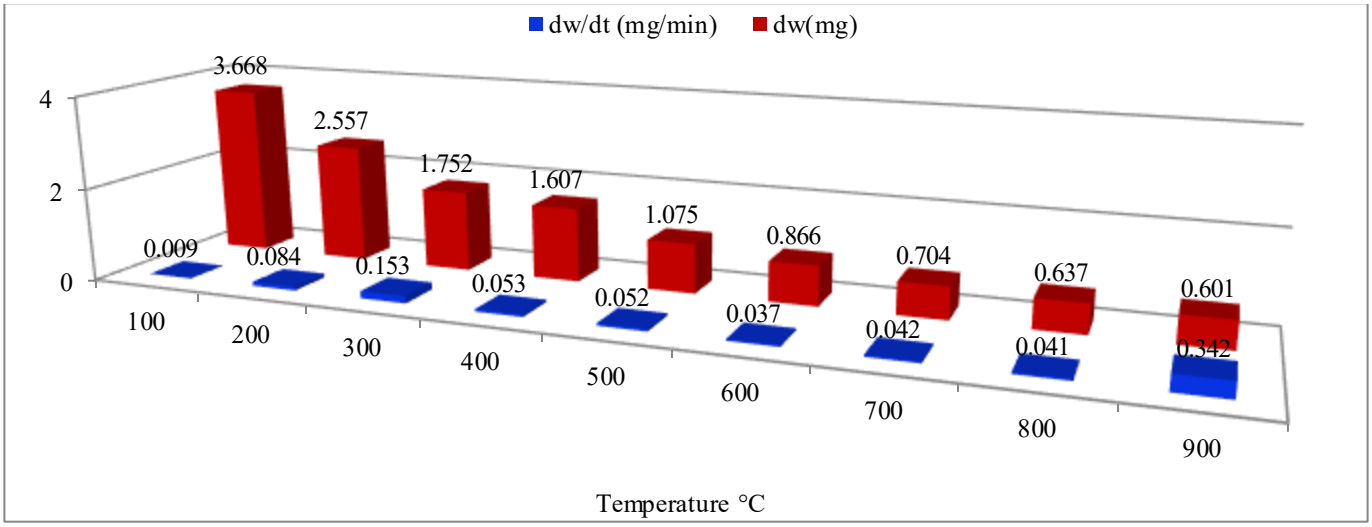

Fig. 6 Thermal mass change and rate of polymer

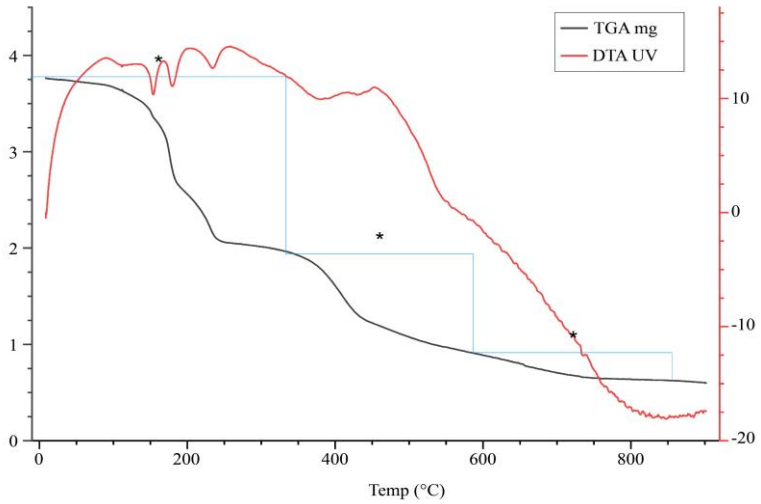

Fig. 7 DGA and DTA analysis of the complex compound

Table 2. Analysis of TGA and DTA curves of polymer

№	Temperature	Mass lost, mg (3.765)	Mass loss, %	Amount of energy consumed (µV*s/mg)	Time spent (min)
1	100	0,097	2,57	13,288	10,43
2	200	1,208	32,08	14,374	20,58
3	300	2,013	53,46	13,085	30,65
4	400	2,158	57,31	10,259	40,75
5	500	2,69	71,44	7,411	50,95
6	600	2,879	76,46	-1.658	61,23
7	700	3,061	81,30	-9.168	71,55
8	800	3,128	83,08	-17.063	74,5
9	900	3,164	84,03	-17.368	92,3

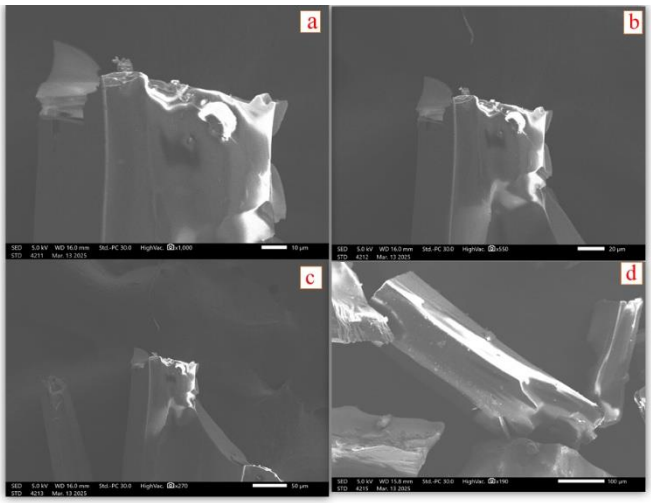

Fig. 8 SEM images of a polymer formed based on 1-hydroxy-2-naphthoic Acid and Cd-acetate salt, at sizes a) 10 µm, b) 20 µm, c) 50 µm, and d) 100 µm

3.5. SEM Analysis

Scanning Electron Microscopic (SEM) analysis of a polymer synthesised from 1-hydroxy-2-naphthoic Acid and Cd-acetate salt. Scanning electron microscopic methods are of great importance in studying the morphology of the newly obtained polymer. The mechanism of formation of the porous structure of the polymer is associated with the nature of the inert diluent and the amount of the caustic agent in the reaction system. In the process of polymer formation, the homogeneity of the morphology of the ring system of the polymer chain plays an important role. In order to fully understand the physicochemical properties of the polymer, it is necessary to study its morphology and structure in Depth. When analysed using a Scanning Electron Microscope (SEM) and energy-dispersive X-ray spectroscopy (EDS), the samples were placed on superconducting carbon adhesive tape, and platinum powder was scattered from above through a platinum plate. Then they were placed in an SEM device. The images were obtained using a JEOL JSM-IT210 model equipped with an EDS system belonging to the InTouchScope™ series from Oxford Instruments. The Scanning Electron Microscopy (SEM) method was used to analyse the surface and morphological structure of the polymer using microscopic features. During SEM analysis, secondary electrons were used at different accelerating voltages (5-20 kV). Each voltage level was focused on studying different aspects of the material, and these magnification levels allowed us to determine the material's fine structure, porosity, and general morphological properties (Figure 8).

a) At the magnification level of 10 µm, the fine structures of the polymer, including the pore system and their distribution, are visible.

b) At the magnification level of 20 µm, the general features of the polymer structure are visible.

c) At The slightly enlarged view compared to 10 µm allows us to determine, for example, the presence of relatively large pores or aggregates.

d) At the magnification level of 50 µm, the broad shapes and structure of the polymer are shown, but small details or structures are lost.

This type of image allowed us to evaluate the bulk properties of the sample, mainly.

At the magnification level of 100 µm, the general structure of the polymer and large structures are visible. It helps to assess the overall shape and orientation of the entire structure rather than small elements. SEM images of the synthesised polymer show a crystalline structure, which is a characteristic of polymer compoundsIn this analysis, the composition of the polymer synthesised from 1-hydroxy-2-naphthoic Acid and Cd acetate salt was studied, and the following elements were identified from the EDS spectrum:

Carbon (C) - 0.28 keV (C-K)

The carbon peak was observed at 0.28 keV, which corresponds to the organic part of the polymer. 1-Hydroxy-2-naphthoic Acid is the primary carbon source and contains aromatic rings and functional groups. A high-intensity C-K peak in the spectrum confirms that the polymer is rich in carbon.

Oxygen (O)—0.53 keV (O-K)

The oxygen peak is located at 0.53 keV, indicating the presence of carboxyl (-COOH) and hydroxyl (-OH). Groups. These groups play a crucial role in the polymer structure and provide evidence of their binding to acidic compounds.

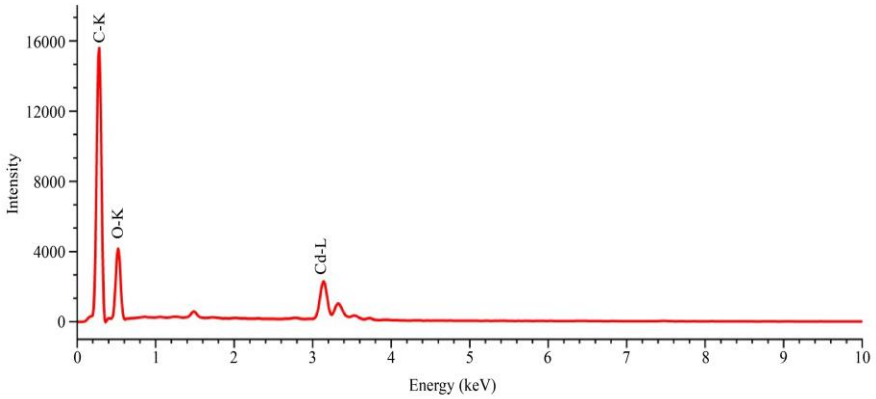

Fig. 9 EDS analysis of polymer composition

Cadmium (Cd)-3.13 keV and 3.38 keV (Cd-L series). The main L-series peaks of cadmium are observed at 3.13 keV and 3.38 keV. These peaks confirm the integration of Cd ions into the polymer. The presence of Cd-L spectral lines indicates that cadmium acts as a Cd (II) coordination centre and aids in forming the polymer network (Figure 9). The quantitative composition of the elements in the polymer was studied in detail using Energy Dispersive X-ray Spectroscopy (EDS) analysis. According to it, the high presence of carbon (C-K, 55.26 ± 0.15 mass% %, 66.83 ± 0.18 atom%) indicates the presence of a two-dimensional coordination polymer structure.

The high concentration of oxygen (O-K, 35.16 ± 0.34 mass% %, 31.93 ± 0.31 atomic% %) indicates the presence of hydroxide and carboxyl in the polymer.

The presence of cadmium (Cd-L, 9.58 ± 0.10 mass% %, 1.24 ± 0.01 atomic% %) proves that the polymer structure consists of metal-organic bonds or is a coordination centre.

These results indicate that the polymer is rich in carbon and oxygen, while cadmium is present in low concentrations. Cadmium ions are integrated into the polymer network, forming coordination bonds (Figure 10).

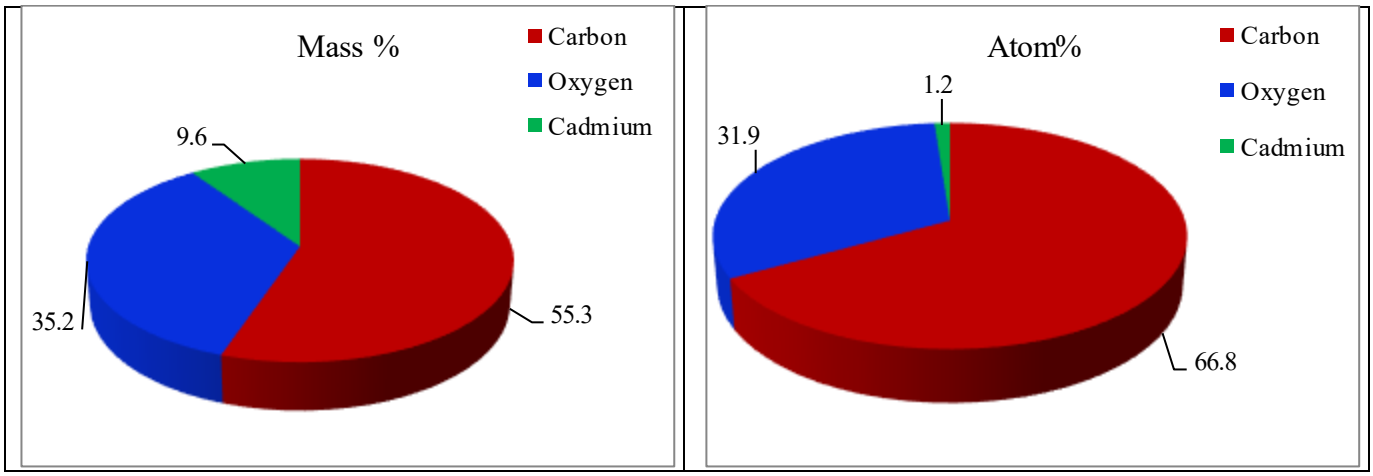

Fig. 10 Results of elemental analysis of a polymer formed from 1-hydroxy-2-naphthoic Acid and Cd acetate salt, (a) mass%, and (b) atomic%

The polymer was taken using a Scanning Electron Microscope (SEM), which shows the microstructure of the polymer surface (Figure 11). The first image is a colourless Scanning Electron Microscopy (SEM) image showing the microstructure of the polymer (Figure 11(a)). The green Cd-L map represents the location of the cadmium (Cd) element. The Cd-L signal is not uniformly distributed in the sample, i.e., some areas have high intensity and others have low intensity. This may indicate that Cd ions or cadmium-based structures (e.g., Cd coordination centres) have formed distinct phases within the polymer (Figure 11(b)). The red C-K map is widely distributed throughout the area because carbon (C) is the main structural element of the polymer. The uniform distribution of the red colour indicates that the polymer matrix has a homogeneous structure (Figure 11(c)). The O-K map shows that the red oxygen (O) element is also evenly distributed and, together with carbon, the polymer structure contains organic groups. The presence of the oxygen element indicates the presence of hydroxyl (-OH), carboxyl (-COOH), or cadmium-bonded oxygen groups (Cd-O) (Figure 11(d)).

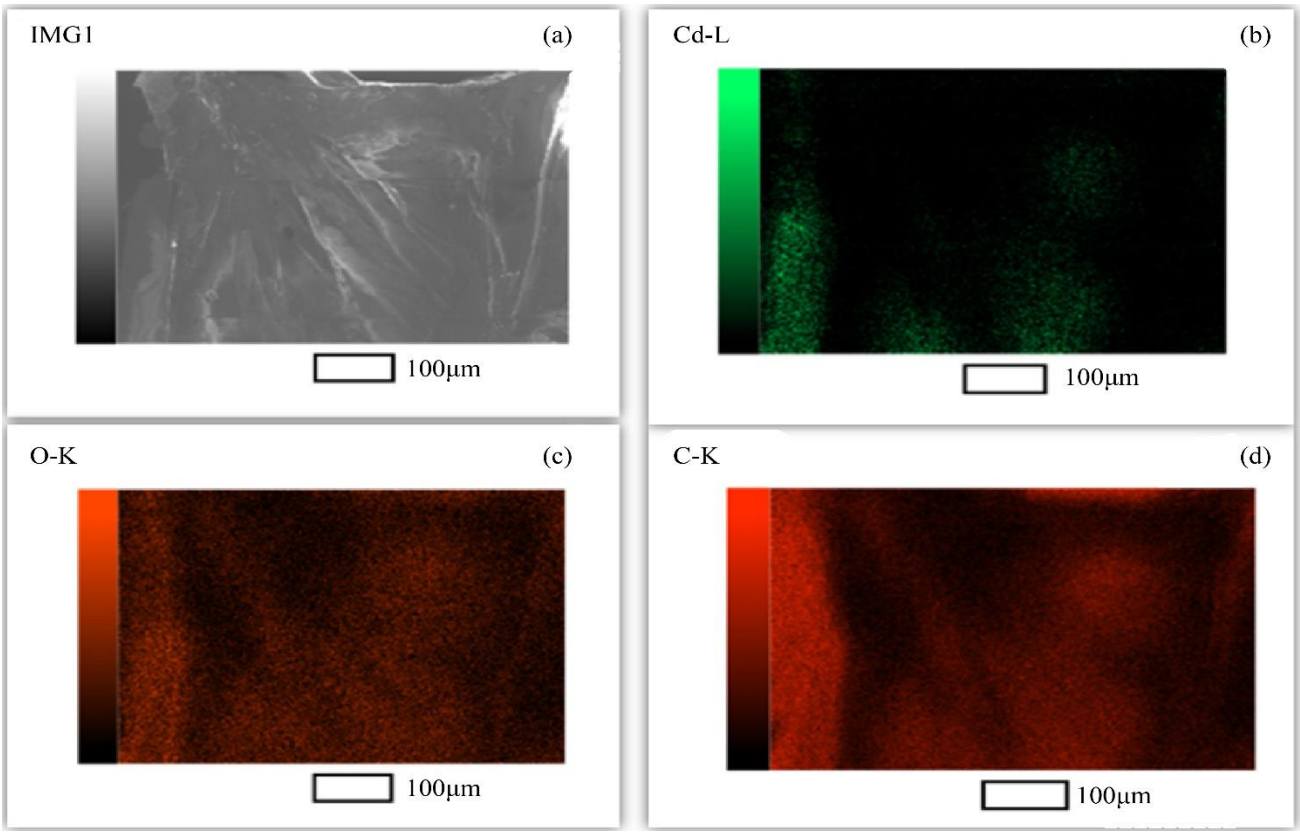

Fig. 11 Mapping colour images of elements in the polymer composition in 100 µm analysis: (a) Sample, (b) Cd-K (cadmium), (c) O-K (oxygen), and (d) C-K (carbon)

3.6. Hirshfeld Surface Analysis

Molecular crystalline structures can be quantitatively analysed using the Hirshfeld surface method. This method shows the displacements at each point on the Hirschfeld surface, corresponding to neighbouring atoms on the outer and inner surfaces. These features were important in studying the selectivity and specificity of intermolecular forces acting on molecular structures. Creating these surfaces involves dividing the space inside the crystal using the Hirschfeld relation.

In this case, the procrystal is effectively determined by a promolecule with an electron density of 0.5. The normalised contact distance, d_{norm}, is calculated by considering the outer and inner sides of the surface as shown below. (Formula 1)

$$d_{norm} = \frac{d_i - r_i^{vdW}}{r_i^{vdW}} + \frac{d_e - r_e^{vdW}}{r_e^{vdW}} \quad (1)$$

Hirschfeld surface analysis demonstrates the complex relationships between the external and internal parts of the crystal structure. The parameter denoted by d_{norm} represents the normalized contact distance. In this case, d_e denotes the distance from the Hirschfeld surface to the nearest external nucleus, and d_i denotes the corresponding distance to the nearest internal nucleus. r^{vdW} represents the van der Waals radius of the atom under consideration.

The d_{norm} parameter is visually represented on the Hirschfeld surface by the color gradient from red through white to blue. Bright red areas indicate intermolecular interactions at distances shorter than the corresponding van der Waals radii, while blue areas indicate intermolecular interactions at distances greater than the corresponding van der Waals radii. The white regions correspond to the total van der Waals radii of the corresponding atoms.

To analyze close-range interactions between neighbouring molecules in crystal lattice structures, researchers used version 17.5 of the Crystal Explorer program [25]. This software was used to study Hirschfeld surfaces of crystalline structures and create corresponding Two-Dimensional (2D) fingerprint diagrams [26].

3.6.1. Hirschfeld Analysis

Hirschfeld surface analysis of the polymer was performed on the coordination polymer assembly using its CIF file. For surface analysis, the asymmetric part of the structure was selected, and the Hirschfeld surface was analysed using Crystal Explorer 17.5 to visualise intermolecular interactions. The d_{norm}, area was determined by calculating the external (de) and internal (di) distances to the nearest nucleus. The standard sizes of the red and blue spots in terms of d_{norm} are -1.2973 and 1.3984, respectively (Figure 12).

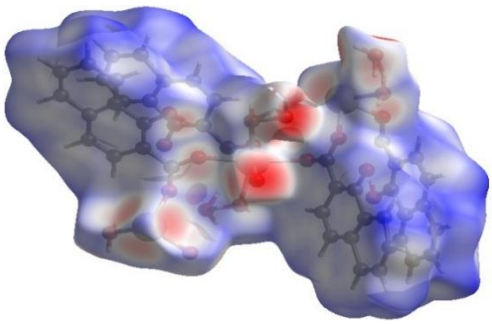

Fig. 12 Total Hirshfeld surface area of a polymer compound

Here, the red colour indicates bonds closer to the sum of van der Waals radii. Blue spots indicate bonds further than the sum of van der Waals radii (Figure 13). According to the d_{norm} of this polymer compound, most red spots on the Hirshfeld surface of the molecule are hydrogen bonds.

The Hirshfeld surface area is S= 749.57 Å² and the volume is V= 959.24 Å³. The interaction of internal particles in the crystal structure was determined using the two-dimensional functions di and the interaction of the crystal surface.

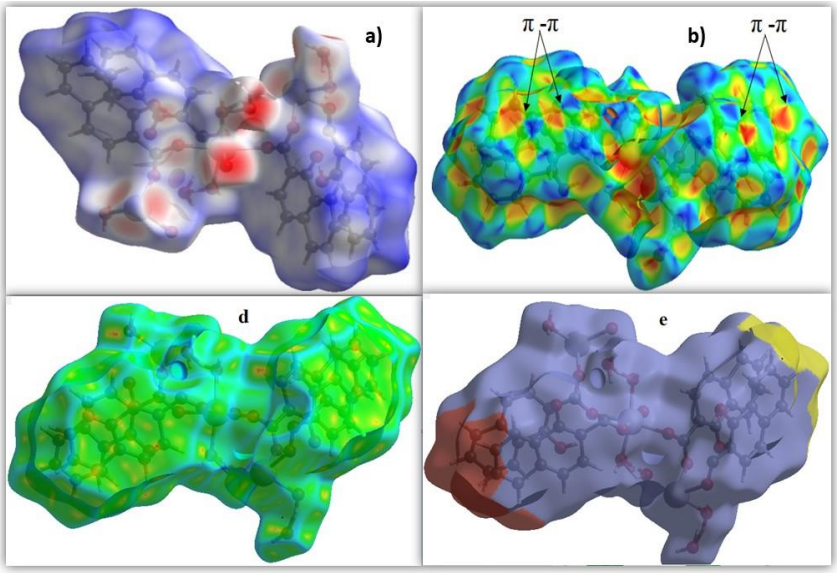

Fig. 13 Hirshfeld surface (a), Shape index (b), Curvedness (c), and Fragment patches (e)

According to the results presented in Figure 14 [27], two-dimensional fingerprint plots obtained with the de and di functions show the contribution of individual interactions to the formation of crystal packing. The fingerprint area shows that H…H interactions contribute the most to surface interactions, typical for molecules dominated by oxygen atoms. Thus, analysis of the Hirshfeld surface reveals that H…H (47.1%), O…H/H…O (23.5%), H…C/C…H (4.7%), Cd…O/O…Cd (3.8%), O…O (5.9%), O…C/C…O (4.7%), Cd…H/H…Cd (0.7%) and C…C (9.6%) interactions contribute to crystal packing. Thus, from the Hirshfeld surface analysis, it is clear that the main part of the interactions is H…H (47.1%) and O…H/H…O (23.5%). These interactions contribute significantly to the crystallinity and the distance between atoms.

The diagram below shows the Hirshfeld fingerprint distribution of a polymer, indicating the percentage of different molecular interactions in the crystal lattice. Hirshfeld surface analysis is an important tool for identifying and quantifying covalent interactions in crystalline materials, and this diagram shows which interactions dominate the structure of the polymer. This diagram shows that hydrogen bonds (O...H), van der Waals forces (H...H), and π-π stacking (C...C) play a major role in the crystal structure of the polymer. This information is important for understanding the physicochemical properties of the material and determining its future applications (Figure 15).

The distribution of element atoms on the polymer's internal and external Hirschfeld surfaces formed from L1 and cadmium salt is analysed. In the inner part of the surface, hydrogen (H) is 59.5% and plays a major role in intermolecular interactions. This shows high H...H and H...O interactions, indicating hydrogen bonds. Oxygen (O) is 20.9% and is an important part of the inner surface.

The presence of carbon (C) is 15.0%, which may reflect π-π stacking interactions. Cadmium (Cd) is 4.6%, indicating a metal-organic framework (MOF) or a polymer complex. In the outer part of the surface, hydrogen (H) is 63.6%, which indicates the strength of hydrogen-related interactions in the crystal lattice. Oxygen (O) is 22.8%, carbon (C) is 13.6%, and cadmium (Cd) is 0%. Metal atoms do not contribute to the outer surface, indicating that Cd is more strongly bound to the inner surface. Analysis of the internal surface reveals that

hydrogen is the most dominant element, comprising approximately 60% of the Hirshfeld surface, which indicates the importance of intermolecular hydrogen bonds. Oxygen and carbon also play significant roles, with their contributions being 20.9% and 15.0%, respectively.

Cadmium is characteristic only of the internal surface and accounts for a 4.6% share. The confinement of cadmium ions to the internal surface confirms that the Cd ions in this polymer are located in the interior of the crystal lattice. (Figure 16)

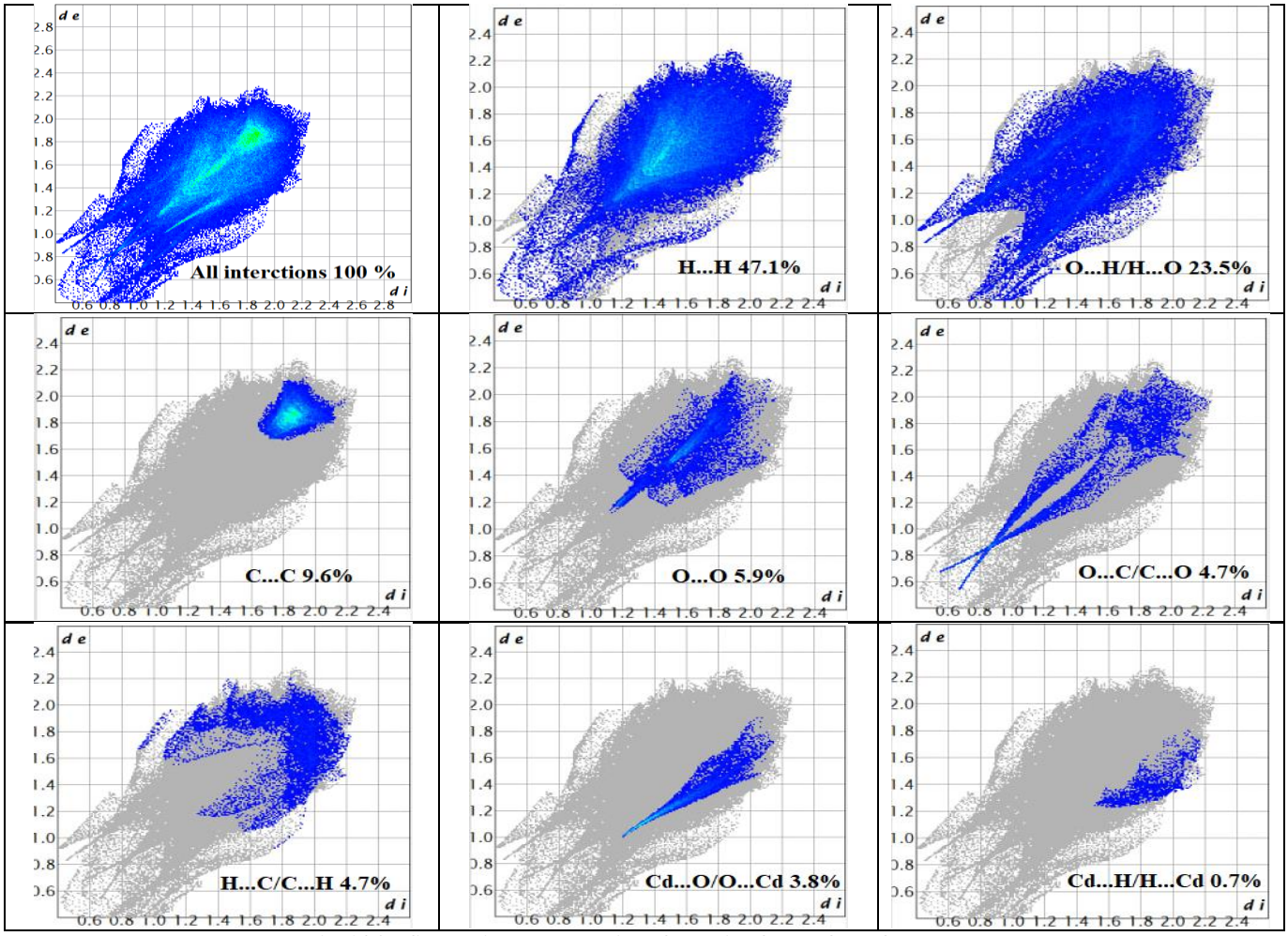

Fig. 14 2D fingerprint representation of the Hirshfeld surface of a polymer

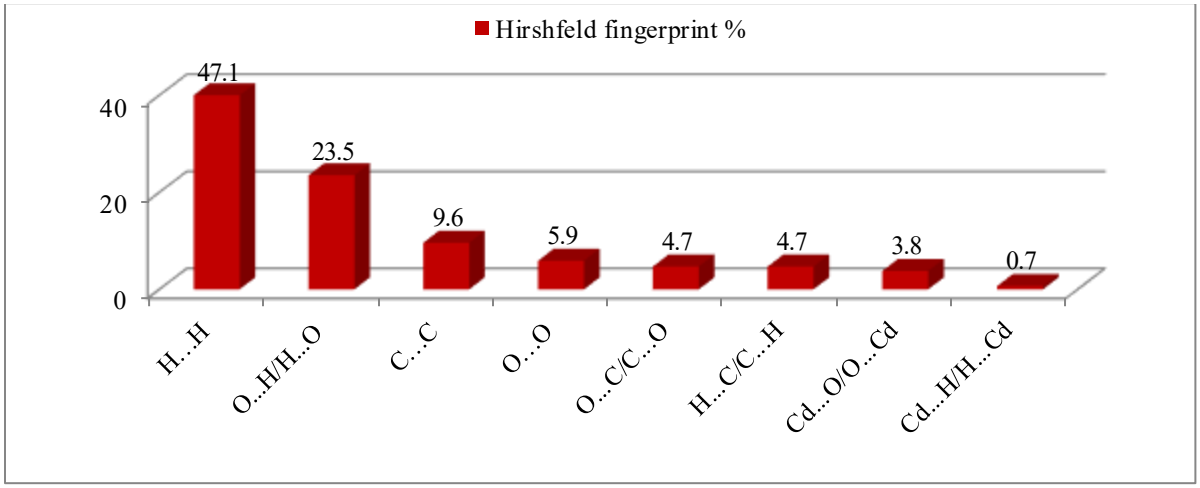

Fig. 15 Hirshfeld fingerprint distribution of a polymer

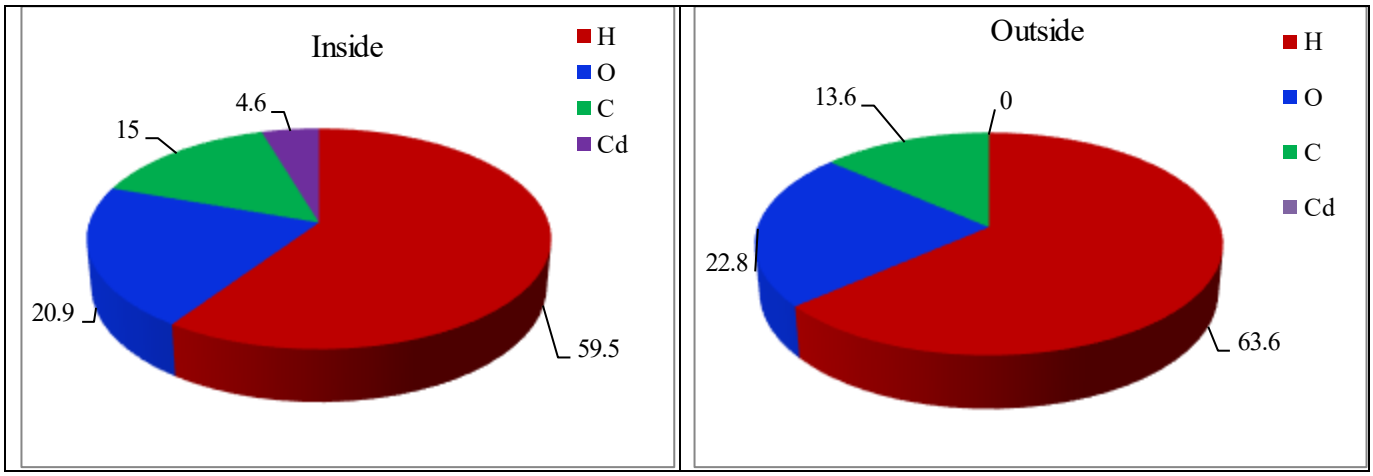

Fig. 16 Contribution of atoms of the same element inside and outside the surface to the formation of the Hirschfeld surface and their differences

3.7. X-Ray Diffraction (XDR) Analysis

In this study, the structure of a polymer formed from L1 and Cd acetate salt was analysed using an X-ray diffractometer (Rigaku's MiniFlex 600 X-ray diffractometer). XRD analysis was performed using Cu-Kα radiation (λ = 1.5406 Å) in the range of 2θ = 3° to 90°, with a step of 0.02° and a time of 1 second at each point. The following main peaks were observed in the obtained XRD spectrum (Figure 17). The horizontal axis is the diffraction angle in degrees (°), the vertical axis is the relative intensity (arb. Units-arbitrary units), and the numbers above the peaks are the crystal lattice spacing, given in nanometers (nm).

XRD analysis results. 2θ = 4.86° (d = 1.815 nm) – This peak indicates the polymer has a layered structure. Such peaks are found in metal-organic frameworks (MOFs) or hydrated coordination polymers. 2θ = 10.46° (d = 0.844 nm) – This peak may be associated with carboxylate ($-COO^-$) groups.

The carboxylate groups are likely coordinated with Cd(II). 2θ = 12.24° (d = 0.722 nm) –This peak indicates that the aromatic rings are arranged in an orderly manner in the crystal lattice. Such diffraction signals appear when they are present in the composition of naphthenic acids or benzene derivatives. 2θ = 14.906° (d = 0.593 nm) – This peak may indicate Cd-organic coordination bonds. When Cd(II) ions are bound to organic ligands, peaks are formed at certain diffraction angles. This confirms that it is a coordination polymer or MOF. 2θ = 26.54° (d = 0.335 nm) – This peak can be associated with Cd-O bonds. Such a peak in materials synthesised based on Cd(II) indicates the presence of CdO. If Cd(II) oxidation occurred during the synthesis process, this peak confirms this. 2θ = 52.409° (d = 0.174 nm) – High 2θ values are usually characteristic of ordered crystal structures with short distances. The carboxylate groups are generally coordinated to Cd(II) ions, which confirms that it is a coordination polymer or MOF.

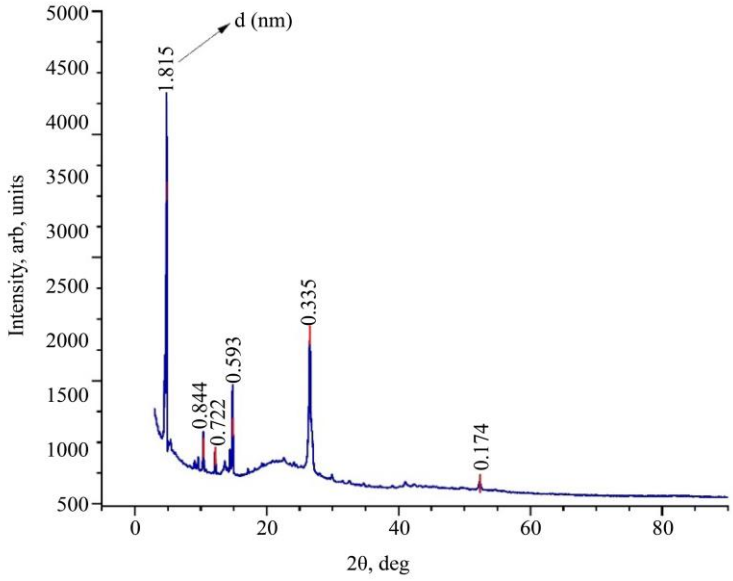

Fig. 17 X-ray diffraction image of the synthesised polymer

X-Ray Diffractometry (XRD) is an important tool for determining the crystallinity of polymers. As can be seen from Table 3, the largest d (Å) value in the XRD spectrum is 18.153 Å (1.815 nm), indicating that the polymer has a layered structure. d = 0.844 nm and 0.722 nm – These peaks may represent coordination bonds between the polymer and metal ions. According to the analysis of the XRD results, the synthesized material has a layered crystal structure, indicating the presence of coordination bonds between Cd(II) ions and the organic ligand.

Table 3. XRD data on the crystal structure of the polymer

№	2nd (deg)	th (°)degree	d (Å)	d (nm)
1	4.864	2.432	18.153	1.815
2	10.463	5.231	8.448	0.844
3	12.240	6,120	7,225	0.722
4	14.906	7.453	5.938	0.593
5	26.548	13.274	3.354	0.335
6	52.409	26,204	1,744	0.174

3.8. Conductometry Analysis

Based on the conducted research, it was established that the compound under study is characterised by a good electrolytic nature [28-31]. The measured molar conductivity of complex 1 in a mixture of ethanol/water (3:2) at a concentration of $1.0\times10^{-}\times 10^{3}$ mol is 3.35 mS at 25°C, which indicates a significant number of ions that provide electric charge transfer in the solution and, therefore, is a high indicator. The total solubility (TDS) value, determined using a TDS metre and amounting to 1.91 ppt, indicates increased dissolved solid particles in the system under study. If the temperature increases, the kinetic energy of molecules increases, which helps to reduce the viscosity of the solution; this, in turn, facilitates the movement of ions, causing an increase in molar conductivity. The finding that TDS also increases with temperature is consistent with the fact that as temperature increases, the solubility of solids generally increases. Thus, at higher temperatures, more dissolved ions and other solids can be present in solution, which will be reflected in the TDS reading (Table 4, Figure 18).

Table 4. Dependence of molar conductivity on the temperature of the polymer

T, °C	Polymer	
	Molar conductivity, mS	TDS, ppt
25	3.35	1.91
35	3.38	1.93
40	3.41	1.90
45	3.45	1.92
50	3.58	1.94
55	3.62	1.96

Successive measurements of solutions with decreasing concentrations show a gradual decrease in molar conductivity. It is important to note that these changes in conductivity are quite significant. A similar dependence is observed in TDS values. As the electrolyte concentration decreases, the number of freely moving ions also decreases, which leads to a decrease in conductivity. This is especially true for strong electrolytes that completely dissociate, since most of their conductivity is directly related to the number of free ions. In a system where the electrolyte completely dissociates, a decrease in concentration also leads to a decrease in the total number of available ions, which will also be reflected in the TDS value. The study results demonstrate that the compound under study is a strong electrolyte with high solubility and the ability to conduct electric current (Table 5, Figure 19).

Table 5. Dependence of molar conductivity on the concentration of polymer

C, mol/m³	Polymer	
	Molar conductivity, mS	TDS, ppt
0.05	4.79	2.65
0.001	4.05	2.03
0.0005	2.96	1.08
0.0001	1.01	0.50
0.000005	0.84	0.08

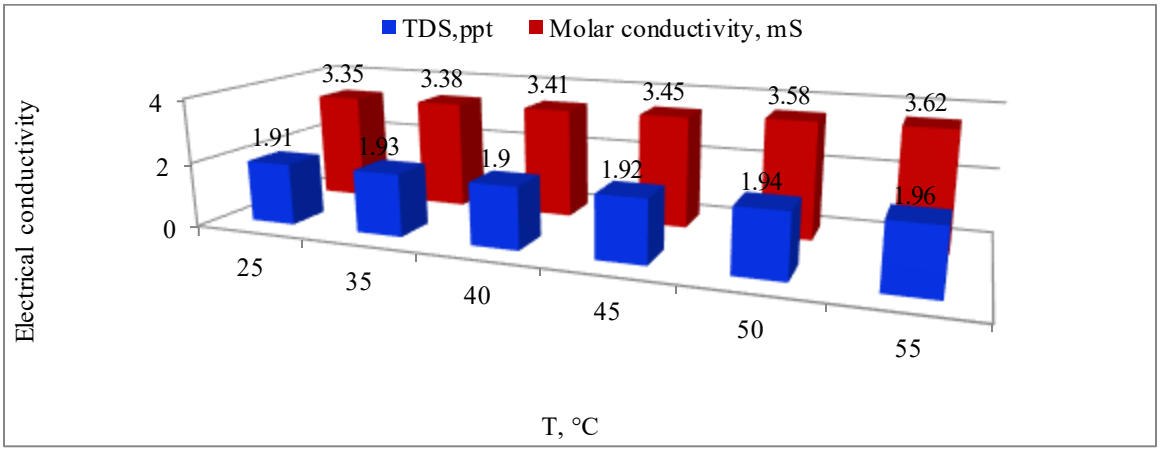

Fig. 18 Comparative analysis of the dependence of the molar conductivity of polymer on temperature

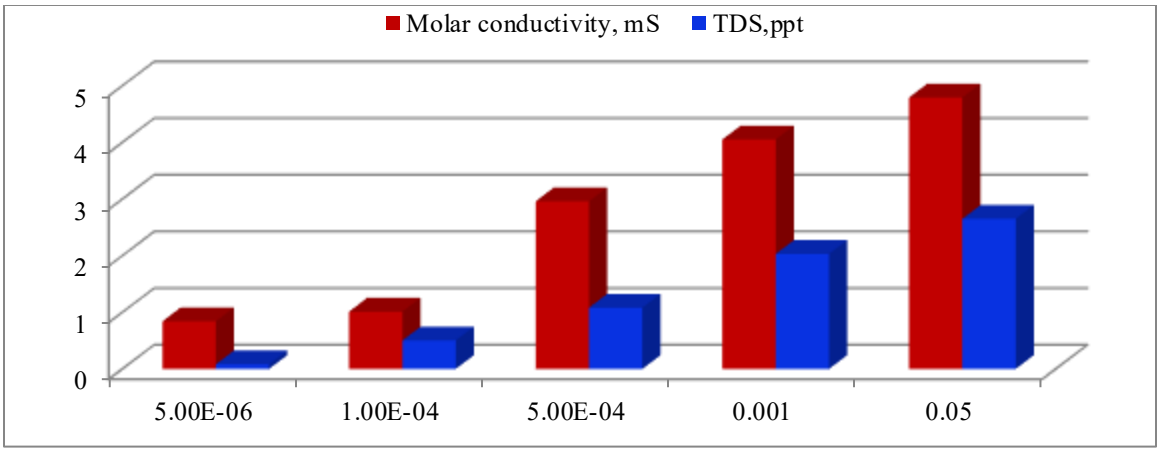

Fig. 19 Comparative analysis of the dependence of the molar conductivity of the polymer on concentration

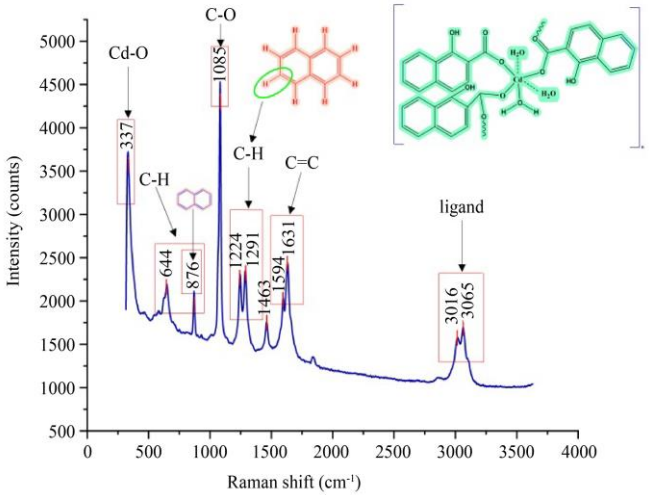

Fig. 20 Raman spectrum of a polymer compound

3.9. Raman Spectral Analysis

Raman spectroscopy was employed to investigate the structure of the coordination polymer synthesised from 1-hydroxy-2-naphthoic acid and $Cd(CH_3COO)_2 \cdot 2H_2O$. The spectrum was recorded in the 100-3500 cm^{-1} range, and the primary vibration peaks were identified. The peak at 337 cm^1 corresponds to the Cd-O bond. Peaks at 644 and 876 cm^{-1} are attributed to vibrations in the aromatic ring and C-H bonds, respectively. Notably, the peak at 876 cm^{-1} confirms the presence of a naphthalene ring. The peak at 1085 cm^{-1} indicates the presence of a C-O bond. Peaks at 1242 and 1291 cm^{-1} are associated with C-H bonds in the aromatic ring. The peak at 1465 cm^{-1} signifies that the carboxylate group is coordinated to the Cd (II) ion. Peaks at 1594 and 1631 cm^{-1} indicate the presence of C=C bonds. Peaks at 3016 and 3065 cm^{-1} demonstrate the vibrations of aromatic C-H bonds and confirm the preservation of the ligand structure. According to the results of Raman analysis, it was determined that Cd (II) ions in the polymer are bound to oxygen-containing groups, and the aromatic ring structure is Maintained. This indicates that the polymer possesses a stable structure (Figure 20).

4. Conclusion

The structure of a novel coordination polymer synthesised from cadmium acetate and 1-hydroxy-2-naphthoic Acid was elucidated using X-ray diffraction data obtained from Rigaku MiniFlex 600 diffractometry and Hirschfeld surface analysis. The physicochemical properties of the polymer were evaluated using TGA/DTA thermal analysis, UV-Vis spectroscopy, CHNS/O elemental analysis, and EDS techniques. SEM imaging and X-ray spectroscopy enabled the determination of its morphological characteristics and elemental composition. Conductometric measurements revealed the polymer's electrical conductivity properties. Based on the results of the analysis, a precise structural formula for the obtained polymer was proposed, and a CCDC Deposit Number was acquired.

Acknowledgments

The authors express their deep gratitude to Termez State University and the Institute of General and Inorganic Chemistry of the Academy of Sciences of Uzbekistan for their support and the scientific environment and research facilities they provided.

References

[1] Abdullaev Ahrorjon Khabibjonovich et al., "Two Dimensional Coordination Polymer of Pb (II) Complex with M-Sulfanilic Acid: Synthesis, Characterization, Electrical Conductivity, Adsorption Properties and Hirshfeld Surface Analysis," *Adsorption*, vol. 31, no. 2, 2025. [CrossRef] [Google Scholar] [Publisher Link]

[2] Claudio Pettinari et al., "Application of Metal - Organic Frameworks," *Polymer International*, vol. 66, no. 6, pp. 731-744, 2017. [CrossRef] [Google Scholar] [Publisher Link]

[3] Fangyu Ren, and Pengfei Ji, "Recent Advances in the Application of Metal - Organic Frameworks for Polymerization and Oligomerization Reactions," *Catalysts*, vol. 10, no. 12, pp. 1-25, 2020. [CrossRef] [Google Scholar] [Publisher Link]

[4] Xiang Zhao et al., "Metal - Organic Frameworks for Separation," *Advanced Materials*, vol. 30, no. 37, pp. 1-103, 2018. [CrossRef] [Google Scholar] [Publisher Link]

[5] Bernhard V.K.J. Schmidt, "Metal-Organic Frameworks in Polymer Science: Polymerization Catalysis, Polymerization Environment, and Hybrid Materials," *Macromolecular Rapid Communications*, vol. 41, no. 1, pp. 1-28, 2020. [CrossRef] [Google Scholar] [Publisher Link]

[6] Dimitrios Giliopoulos et al., "Polymer/Metal Organic Framework (MOF) Nanocomposites for Biomedical Applications," *Molecules*, vol. 25, no. 1, pp. 1-28, 2020. [CrossRef] [Google Scholar] [Publisher Link]

[7] A. Dieter Schlüter, Thomas Weber, and Gregor Hofer, "How to Use X-ray Diffraction to Elucidate 2D Polymerization Propagation in Single Crystals," *Chemical Society Reviews*, vol. 49, no. 15, pp. 5140-5158, 2020. [CrossRef] [Google Scholar] [Publisher Link]

[8] Austin M. Evans et al., "Controlled n-Doping of Naphthalene-Diimide-Based 2D Polymers," *Advanced Materials*, vol. 34, no. 22, pp. 1-22, 2022. [CrossRef] [Google Scholar] [Publisher Link]

[9] Liyuan Xiao, Zhenlu Wang, and Jingqi Guan, "2D MOFS and their Derivatives for Electrocatalytic Applications: Recent Advances and New Challenges," *Coordination Chemistry Reviews*, vol. 472, 2022. [CrossRef] [Google Scholar] [Publisher Link]

[10] Alexandre Abhervé et al., "Graphene Related Magnetic Materials: Micromechanical Exfoliation of 2D Layered Magnets Based on Bimetallic Anilate Complexes with Inserted [Fe III (acac 2-trien)]$^{+}$ and [Fe III (sal 2-trien)]$^{+}$ Molecules," *Chemical Science*, vol. 6, no. 8, pp. 4665-4673, 2015. [CrossRef] [Google Scholar] [Publisher Link]

[11] Bingbing Liu et al., "2D MOF with Electrochemical Exfoliated Graphene for Nonenzymatic Glucose Sensing: Central Metal Sites and Oxidation Potentials," *Analytica Chimica Acta*, vol. 1122, pp. 9-19, 2020. [CrossRef] [Google Scholar] [Publisher Link]

[12] Sukanya Bhunia, Kaivalya A. Deo, and Akhilesh K. Gaharwar, "2D Covalent Organic Frameworks for Biomedical Applications," *Advanced Functional Materials*, vol. 30, no. 27, pp. 1-74, 2020. [CrossRef] [Google Scholar] [Publisher Link]

[13] Pan-Pan Sun et al., "Real-Time Fluorescent Monitoring of Kinetically Controlled Supramolecular Self-Assembly of Atom-Precise Cu_8 Nanocluster," *Angewandte Chemie*, vol. 135, no. 20, 2022. [CrossRef] [Google Scholar] [Publisher Link]

[14] Xiaoxi Ji et al., "A Water-Stable Luminescent Sensor Based on Cd^{2+} Coordination Polymer for Detecting Nitroimidazole Antibiotics in Water," *Applied Organometallic Chemistry*, vol. 35, no. 10, 2021. [CrossRef] [Google Scholar] [Publisher Link]

[15] Dr. Yifan Gu et al., "Host–Guest Interaction Modulation in Porous Coordination Polymers for Inverse Selective CO_2/C_2H_2 Separation," *Angewandte Chemie International Edition*, vol. 60, no. 21, pp. 11688-11694, 2021. [CrossRef] [Google Scholar] [Publisher Link]

[16] Liangying Li et al., "Discrimination of Xylene Isomers in a Stacked Coordination Polymer," *Science*, vol. 367, no. 6603, pp. 335-339, 2022. [CrossRef] [Google Scholar] [Publisher Link]

[17] Zhifen Guo et al., "One-Pot Dual Catalysis of a Photoactive Coordination Polymer and Palladium Acetate for the Highly Efficient Cross-Coupling Reaction via Interfacial Electron Transfer," *Inorganic Chemistry*, vol. 61, no. 5, pp. 2695-2705, 2022. [CrossRef] [Google Scholar] [Publisher Link]

[18] Yingbi Chen et al., "High Selectivity and Reusability of Coordination Polymer Adsorbents: Synthesis, Adsorption Properties and Activation Energy," *Microporous and Mesoporous Materials*, vol. 324, 2021. [CrossRef] [Google Scholar] [Publisher Link]

[19] Aleksej Jochim et al., "Structural Diversity in Ni Chain Coordination Polymers: Synthesis, Structures, Isomerism and Magnetism," *European Journal of Inorganic Chemistry*, vol. 2018, no. 44, pp. 4779-4789, 2018. [CrossRef] [Google Scholar] [Publisher Link]

[20] Yu-Rong Xi et al., "A Set of Cd-Based Metal Coordination Complexes with a Novel Bis (Hydroxyl Naphthoic Acid) Ligand: Syntheses, Structure and Luminescent Properties," *Structure and Luminescent Properties*, pp. 1-25, 2022. [CrossRef] [Google Scholar] [Publisher Link]

[21] Xiao-Ling He et al., "New Photoluminescent Zn (II)/Cd (II) Coordination Polymers for Laryngeal Carcinoma Therapy," *Chemical Papers*, vol. 76, no. 5, pp. 2875-2882, 2022. [CrossRef] [Google Scholar] [Publisher Link]

[22] K. Venkataraman, *The Chemistry of Synthetic Dyes*, Volume V, Academic Press, New York, 1971. [Online]. Available: https://api.pageplace.de/preview/DT0400.9780323142953_A23647633/preview-9780323142953_A23647633.pdf

[23] Shadia A. Elsayed et al., "New Complexes of 2-Hydroxy-1-Naphthoic Acid and X-ray Crystal Structure of [Pt (hna)$(PPh_3)_2$]," *Journal of Molecular Structure*, vol. 1036, pp. 196-202, 2013. [CrossRef] [Google Scholar] [Publisher Link]

[24] Yusufjon Eshkobilovich Nazarov et al., "Bis (8-hydroxyquinolinium) Naphthalene-1, 5-Disulfonate Tetrahydrate," *IUCrData*, vol. 9, no. 6, 2024. [CrossRef] [Google Scholar] [Publisher Link]

[25] F.S. Narmanova et al., "Synthesis, Structure, Hirshfeld Surface Analysis, and Molecular Docking Studies of the Cu (II) complex with 3-Nitro-4-Aminobenzoic Acid," *Structural Chemistry*, vol.35, no. 5, pp. 1641-1648, 2024. [CrossRef] [Google Scholar] [Publisher Link]

[26] F.S. Narmanova et al., "The Structure and Hirshfeld Surface Analysis of the 4-Amino 3-Nitrobenzoic Acid Triclinic Polymorph," *Structural Chemistry*, vol. 35 no. 3, pp. 953-960, 2024. [CrossRef] [Google Scholar] [Publisher Link]

[27] Mark A. Spackman, and Dylan Jayatilaka, "Hirshfeld Surface Analysis," *CrystEngComm*, vol. 11, no. 1, pp. 19-32, 2009. [CrossRef] [Google Scholar] [Publisher Link]

[28] Yokubjon Bozorov et al., "Ion Exchange Membranes in Environmental Applications: Comprehensive Review," *Chemosphere*, vol. 377, 2025. [CrossRef] [Google Scholar] [Publisher Link]

[29] Abror Nomozov et al., "Synthesis of Corrosion Inhibitors Based on (Thio)Urea, Orthophosphoric Acid and Formaldehyde and their Inhibition Efficiency," *Baghdad Science Journal*, vol. 22, no. 4, pp. 1-15, 2025. [CrossRef] [Google Scholar] [Publisher Link]

[30] Mokhichekhra Shaymardanova et al., "Studying of The Process of Obtaining Monocalcium Phosphate based on Extraction Phosphoric Acid from Phosphorites of Central Kyzylkum," *Baghdad Science Journal*, vol. 21, no. 12, pp. 1-21, 2024. [CrossRef] [Google Scholar] [Publisher Link]

[31] Abror Kh. Ruzmetov et al., "Synthesis, Crystal Structure and Hirshfeld Surface Analysis of Binuclear Cu (II) Complexes from O/P-Hydroxybenzoic Acid with Ethanol and Water Solution of Monoethanolamine," *Polyhedron*, vol. 242, 2023. [CrossRef] [Google Scholar] [Publisher Link]